J. Chem. Sci. Vol. 125, No. 3, May 2013, pp. 679–686.

TPR and TPD studies of effects of Cu and Ca promotion on Fe–Zn-based Fischer–Tropsch catalysts

OLUSOLA O JAMES[a,b,*], BISWAJIT CHOWDHURY[b] and SUDIP MAITY[a,*]

[a]Liquid Fuels Section, Central Institute of Mining and Fuels Research (CIMFR), Digwadih Campus, PO FRI 828 108, Dhanbad, India

[b]Applied Chemistry Department, Indian School of Mines, Dhanbad 826 004, India

e-mail: sudip_maity@yahoo.com; jamesoladele2003@yahoo.com

MS received 2 August 2012; revised 4 October 2012; accepted 8 November 2012

Abstract. Temperature-programmed reduction (TPR) and temperature-programmed desorption (TPD) were used to study the effects of Cu and Ca promotion on Fe–Zn-based Fischer–Tropsch catalysts. The reduction temperature for $Fe_2O_3 \rightarrow Fe_3O_4$ was unaffected by Ca addition but decreased when promoted with Cu. Fe–Zn promoted with Cu and Ca showed even much lower reduction temperature for $Fe_2O_3 \rightarrow Fe_3O_4$. Ca promotion enhances carburization and increases surface acidity and basicity of the Fe–Zn oxide precursor. While Cu inhibits carburization and decreases the surface acidity and basicity of the Fe–Zn oxide precursor. The implications of these effects on the application of catalysts for FT are discussed.

Keywords. Iron-based Fischer–Tropsch catalysts; TPR; TPD; carburization.

1. Introduction

There has been global renaissance of Fischer–Tropsch synthesis (FTS) in the energy industry in recent times. The renewed interest in FTS is to a large extent due to anticipated decline in crude supply in the near future; and to a lesser extent due to environmental and climate change concerns.[1–3] FTS provides means to obtain liquid fuels from other carbonaceous resources (natural gas, coal and biomass). From the 1920s, when it was discovered, and early 1990s, commercial developments of FTS were driven state policies. Germany and South Africa used FTS to generate part of their transportation fuel needs during World War II and apartheid regime, respectively.[4,5] Commercial FTS operations received further boost since two decades ago due to discoveries and monetisation of natural gas reserves into liquid fuels.[6] For security of liquid fuel supplies, coal-based FTS operations is also receiving attention in coal-rich countries.[7,8] Towards low-carbon foot print process, biomass-based FTS is equally receiving increasing attention as renewable carbon resources.[9,10] From 1990s till date, more commercial FT plants had been constructed and many more are under various stages of commencement of operations.[1]

Catalysts are central to the process economy of FTS operations and there are many studies on FTS catalysts, yet there are still room for further improvement in this area. Commercial FT catalysts are based on iron and cobalt. At present, there are two modes of commercial FTS operations: high-temperature mode (HTFT) which is carried out at 300–350°C using Fe-based catalysts and low-temperature mode (LTFT) at 200–250°C using either Fe- or Co-based catalysts.[5] Cobalt catalysts are generally more active than Fe-based catalysts. Fe-based catalysts are water gas shift (WGS) reaction active. The WGS reaction is unwarranted in FTS with syngas of H_2/CO ratio 2. Hence cobalt-based catalysts are preferred for LTFT operation mode.[11] However, cobalt metal is about 250–1000 times more expensive than the iron.[12] Moreover, analysis of ease of refining of syncrudes to on-specification diesel fuels indicated that iron-based LTFT syncrude poses less refining challenges compared with cobalt-based LTFT.[13] Thus, design of iron-based FT catalysts having comparable activity to cobalt catalysts is desirable for enhanced process economy.

Syngas feeds directly from coal and biomass gasifiers are hydrogen deficient (H_2/CO < 2). LTFT using such syngas sources requires conditioning of the H_2/CO ratio via *ex situ* WGS reaction prior to the FTS step. This step is particularly necessary for cobalt-based LTFT because cobalt catalysts have very WGS activity. For iron-based LTFT, a catalyst with sufficiently high WGS activity can adjust the H_2/CO ratio *in situ* (concurrently)

*For correspondence

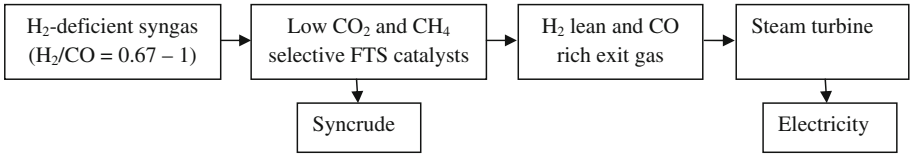

Scheme 1. Flow chart of a coal-based syncrude and electricity co-production process.

with the FTS step. In the two cases, part of the CO is thrown out as CO_2 to adjust the H_2/CO ratio. This has implications on well-to-wheel ratio and carbon utilization of the process.[1] It has been shown that co-production of electricity along with liquid fuels has an economic advantage over a purely liquid fuel Coal-to-Liquid (CTL) or Biomass-to-Liquid (BTL) plants.[14] In a recent review report,[15] we had proposed a scheme for optimized electricity generation and liquid fuel production (scheme 1). Critical requirements for a catalyst for the FTS section in the scheme are: low cost, low CO_2 and CH_4 selectivity. This report is part of our quest for catalysts that meet the requirements.

The low cost requirement is readily met by iron, however, low CO_2 selectivity is not traditional to iron-based FT catalysts. A report by Li *et al.*[16] has showed the possibility of Fe-based catalyst that have comparable activity with cobalt catalysts. These authors argued that the lower apparent FTS rate on Fe-based catalysts is to some extent due to the lower dispersion of their active components. It was advanced that an increase in the surface area and in the density of active sites during synthesis and during the initial stages of use in synthesis gas may bring Fe-based catalysts into the range of productivity and reaction conditions typical of Co-based catalysts. They showed that high surface area Fe–Zn–K–Cu oxide precursors prepared using a solvent replacement method, displayed hydrocarbon synthesis rates (per catalyst mass or volume) compared to those on Co-based catalysts under identical reaction condition ($T = 473$ K, $P = 2.0$ MPa and $H_2/CO = 2$). In addition, Fe–Zn–Cu–K was reported to have the following desirable properties: high syngas conversion and C_{5+} selectivity; low CH_4 and CO_2 selectivity compared to bench mark iron FT catalyst and the selectivity of the catalyst is weakly affected by temperature and syngas composition. In our review report,[15] we commented that Zn/Fe ratio has a link with the CO_2 selectivity of Fe–Zn–Cu–K. Also, we submitted that key parameters for FTS catalyst design are hydrogenation, acidic and basic sites. While investigations of Li *et al.* had been on catalysts with Zn/Fe ratio 0.1 and syngas feed of $H_2/CO = 2$, towards catalysts that will use syngas feed $H_2/CO \leq 1$, we chose Zn/Fe ratio 0.25 for our study and therefore try to investigate the acid–base properties of the resulting Fe–Zn-based catalysts.

Iron-based catalysts are usually promoted with alkali and copper.[17–20] In the catalyst Fe–Zn–Cu–K, Fe–Zn is the active site precursor while Cu and K are promoters. In an earlier study on Fe–Zn-based FT catalyst, Li *et al.*[21] investigated the effect of Cu and K on the report of the Fe–Zn oxide precursor. The authors found that Cu enhanced reduction of the iron oxide in hydrogen and K increase the carburization of the oxide precursors. Cu is also found to increase CH_4 and the paraffin content in FTS products, but the additional presence of K inhibits these effects. The presence of Cu and K synergistically promotes nucleation of active sites thereby increasing FTS rates on the catalyst. However, K and Cu both increase CO_2 selectivities during FTS reactions on catalysts based on Fe–Zn oxide precursors. Several reports have indicated that the presence Ca can reduce CO_2 selectivity of Fe-based FT catalysts.[22–24] We consider that promotion of Fe–Zn oxide with Ca in place of K will further reduce CO_2 selectivity of Fe catalyst based on Fe–Zn oxide precursors. Here, we report the results of effects Ca and Cu promotion on the reduction, carburization, and surface acid–base properties of Fe–Zn-based Fischer–Tropsch catalyst.

2. Experimental

2.1 *Catalyst preparation*

The catalyst compositions in atomic ratio are presented in table 1. The catalysts were prepared by co-precipitation. Na_2CO_3 (2.5 M) was added drop-wise to a solution (0.5 M) containing the nitrates salts of the metals in the desired ratio to pH = 8.5 ± 0.5 while temperature was maintained between 70–80°C under mixing with the aid of a motor stirrer. The resulting precipitates were washed with double distilled water

Table 1. Atomic ratios of the constituent metal of the catalysts.

Catalyst	Atomic ratio
Fe–Zn	100 : 25
Fe–Zn–Cu	100 : 25 : 2
Fe–Zn–Ca	100 : 25 : 1.5
Fe–Zn–Cu–Ca	100 : 25 : 2 : 1.5

till the filtrates are nitrate-free. The precipitates were dried overnight and calcined at 400°C for 4 h. The compositions of the catalysts were re-verified by ICP-OES (Thermo ICAP 6300 Duo) analysis of the calcined samples. The ICP-OES results in ppm were divided by atomic mass of the respective constituent metals. The resulting ratios were converted into atomic ratio by multiplying the ratios through a factor which gives proportion of Fe as 100.

2.2 *N_2 physisorption*

Specific surface areas of catalysts were determined using Micromeritic Chemisorb 2720. The surface area was determined using the Brunauer–Emmett–Teller (BET) equation by the single point method from amount of desorbed nitrogen after physisorption at liquid-nitrogen temperature.

2.3 *X-ray diffraction*

XRD patterns are recorded at room temperature on a D8 ADVANCE (BRUKER AXS, Germany) diffractometer using CuK_α radiation with parallel beam (Gobel Mirror). The catalysts are ground to fine powder prior to measurement. The scans are recorded in the 2θ range between 10 and 75° using step size of 0.02° and scan speed of 2 s/step. Peaks are identified by search match technique using DIFFRAC^{plus} software (BRUKER AXS, Germany) with reference to the JCPDS database.

2.4 *Temperature programmed reduction (TPR)*

TPR and TPD profiles of the catalysts are obtained with ChemiSorb 2720 (Micrometrics, USA) equipped with a TCD detector. The H_2-TPR profiles are obtained by reducing the catalyst samples by a gas mixture of 10% H_2 in Ar with a flow rate of 20 ML/min and the temperature is increased from ambient to 800°C at a rate of 10°C/min. While the CO-TPR are obtained by heating the catalyst samples by a gas mixture of 5.2% CO in He with a flow rate of 20 ML/min and the temperature is increased from ambient to 800°C at a rate of 10°C/min. Hydrogen consumption in the TPR peak area was evaluated by peak area of CuO-TPR calibration.

2.5 *Temperature programmed desorption (TPD)*

The TPD was carried out by first reducing a catalyst with H_2 at 400°C for 8 h. The gas flow was then switched to He and temperature raised to 450°C at the rate of 10°C/min and kept at 450°C for 30 min and then cooling to ambient temperature to eliminate adsorbed H_2 from the catalyst surface. NH_3 uptake on the catalyst surface take place when the gas flow was changed to 4% NH_3 in He. The NH_3-TPD profile was obtained by a temperature programme under He with a flow rate of 20 mL/min from ambient temperature to 1000°C at a rate of 10°C/min. CO_2–TPD was obtained by the same procedure using 5.2% CO_2 in He for the CO_2 uptake. The amounts of NH_3 and CO_2 desorbed in the TPD peak area was evaluated by extrapolation from peak area calibrations with by pulses of standard volumes NH_3 and CO_2 in a flow of He.

3. Results and discussion

3.1 *Composition and surface area*

ICP-OES verification of the composition of the catalysts is presented in table 2. The table shows that the calcined catalysts have minimal deviations from intended compositions. Table 2 also shows the surface area of the catalysts. Surface area increases with Ca promotion but shrinks with Cu promotion. The surface area shrinkage effect of Cu dominates the surface area increase effect of Ca in the Cu–Ca co-promoted catalyst.

3.2 *XRD phase analyses*

Fe and Zn, the main components in the catalysts precipitate as hydroxides which were subsequently converted to for α-Fe_2O_3 and $ZnFe_2O_4$ phases after calcination. These phases are evident in the XRD pattern of the catalysts (figure 1). The α-Fe_2O_3 phase transforms into the FTS active sites during activation (carburisation/reduction) prior to FT reaction. But $ZnFe_2O_4$ phase is non-reducible during the activation process. Because $ZnFe_2O_4$ phase is stable under the activation condition, Li *et al.*[16] advanced that it acts as textural promoter by increasing dispersion and prevent sintering of the active sites. The catalyst preparation procedure was carried out on the nitrate salts of the promo-

Table 2. Atomic ratios of the constituent metal of the catalysts.

Catalyst	BET surface area (m^2/g)	Atomic ratio from ICP-OES analysis
Fe–Zn	48	100 : 24.6
Fe–Zn–Cu	40	100 : 24.1: 2.1
Fe–Zn–Ca	50	100 : 24.4 : 1.5
Fe–Zn–Cu–Ca	43	100 : 24.7 : 2.2 : 1.5

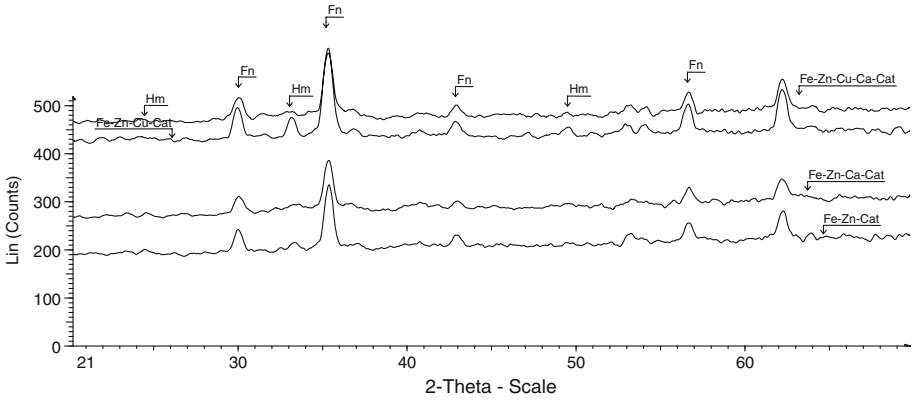

Figure 1. X-ray diffractograms of the catalysts [Hm: Haematite (Fe_2O_3); Fn: Franklinite ($ZnFe_2O_4$)].

ters (Cu and Ca) separately. CuO and $CaCO_3$ phases were obtained as final phase of Cu and Ca, respectively. These phases are expected in the respective promoted catalysts. Figure 1 shows no diffraction peaks due to CuO and $CaCO_3$ phases. This may be because they are present in small amount and co-precipitation method of incorporating them lead to efficient dispersion in the Fe–Zn oxide precursor. Cu and alkali ions are usually incorporated into Fe oxide precursors by impregnation technique and same technique had been extended to alkaline metal ions. Luo *et al.*[22] and Pour *et al.*[23] investigated the effect of Ca promotion on FT performance of Fe oxide precursors. Ca ions was introduced into the Fe oxides by impregnation with $Ca(NO_3)_2$. After impregnation, their catalysts were dried and calcined at 350°C and 450°C for 4 h, respectively. Contrary to the expectation of these authors, after calcination the impregnated $Ca(NO_3)_2$ decompose to CaO, it has been shown that $Ca(NO_3)_2$ decomposes only at temperature ≥550°C even in reducing atmosphere.[24,25] Thus, the impregnated $Ca(NO_3)_2$ in the catalysts reported by Luo *et al.* and Pour *et al.* remained unchanged as $Ca(NO_3)_2$. High temperature calcination of the catalyst to unsure decomposition of $Ca(NO_3)_2$ is at the compromise of loss of surface area due to sintering. Tao *et al.*[26] also studied the effect of Ca and K promotion on the FT performance of Fe–Mn oxide precursor. The authors co-precipitated Ca with Fe and Mn. The resulting calcined catalyst was then impregnated with K_2CO_3. While the challenge of high temperature calcination of the catalyst is absent, it is difficult to delineate promotion effect of Ca from that of K in that catalyst.

3.3 *H_2-TPR of the catalysts*

H_2-TPR provides insight on the reduction behaviour of the phases in the catalysts. Figure 2 shows the H_2-TPR profiles of the catalysts. The Cu-free catalysts displayed nearly identical H_2-TPR profiles. The profiles can be partitioned into two hydrogen consumption temperature ranges: 80–400°C and >400°C. The peaks in the temperature ranges were assigned to $Fe_2O_3 \rightarrow Fe_3O_4$ and $Fe_3O_4 \rightarrow FeO \rightarrow Fe$ transitions, respectively. Hydrogen consumptions at the peak temperatures as measured by the area under the peaks are shown in figure 3. The reduction peak temperature of the transition, $Fe_2O_3 \rightarrow Fe_3O_4$, was unaffected by Ca promotion. However,

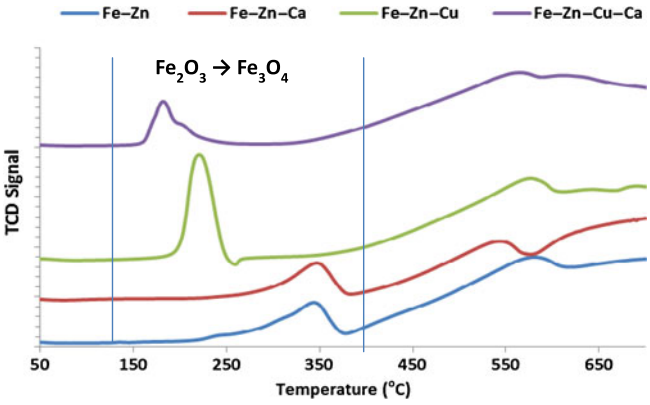

Figure 2. H_2-TPR profiles of the catalysts.

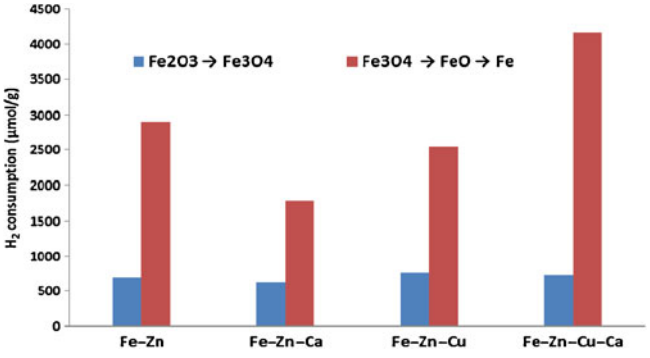

Figure 3. H_2 consumption measured by area under the peak temperatures in the H_2-TPR profiles of the catalysts.

decrease of $Fe_2O_3 \rightarrow Fe_3O_4$ reduction peak temperature is well-known with Cu promotion. Dispersed copper phase (oxides) in the catalyst are reduced to metallic copper nanoparticles at lower temperature. The copper nanoparticles are hydrogen activation sites from which activated hydrogen spilled over to the Fe_2O_3 thereby facilitating reduction to Fe_3O_4 at lower temperature. So, decrease of $Fe_2O_3 \rightarrow Fe_3O_4$ reduction peak temperature of Fe–Zn–Cu by 123°C is readily explained by hydrogen spill-over effect from the copper promoted. $Fe_2O_3 \rightarrow Fe_3O_4$ reduction peak temperature was further reduced by 40°C in the Fe–Zn–Cu–Ca. This may be attributed to enhanced dispersion of copper phase in the catalyst in the presence Ca phase.

As shown in figure 3, hydrogen consumptions in the temperature range of 80–400°C in the four catalysts are very close. The presence of Cu and Ca in the Fe–Zn oxide precursor seems to have synergy effect for the reduction in the temperature range. This shows that the reaction at this stage is identical in the four catalysts. Little difference in the hydrogen consumptions is due to compositional difference with the introduction of Cu and Ca into Fe–Zn oxide precursor. However, hydrogen consumptions at temperature >400°C showed marked differences. The variation may be attributed to the different extent of the two reduction reactions, $Fe_3O_4 \rightarrow FeO \rightarrow Fe$, in the catalysts. $Fe_3O_4 \rightarrow FeO \rightarrow Fe$ transitions are less critical for FTS application compared $Fe_2O_3 \rightarrow Fe_3O_4$ which is an intermediate phase in active site formation during carburization.

3.4 *CO-TPR of the catalysts*

Carburization behaviour of the catalysts was studied by CO-TPR. Figure 4 shows the CO-TPR profiles of the catalysts. Lower peak temperatures in the profiles are not well-resolved. The profiles were divided into four temperature ranges and the CO consumptions in the ranges for each catalyst were presented in figure 5. The figure revealed that Fe–Zn–Ca and Fe–Zn–Cu showed higher and lower total CO consumption, respectively than Fe–Zn. This shows that the presence of Ca in Fe–Zn oxide promote carburization while Cu suppressed it. Carburization promotion of Ca might have masked by Cu in Fe–Zn–Cu–Ca. According to Li *et al.*,[16] Fe_2O_3 reduces to Fe_3O_4 in CO at 270°C and subsequent carburization of Fe_3O_4 occurs at temperature above 270°C. However, at temperatures above 450°C, carburization is accompanied with excessive formation amorphous carbon due to disproportionate CO via Boudouard reaction. Thus, we restrict discussion in this contribution to CO consumption in temperature ranges of α and β (i.e., below 400°C) since this range is important for selecting optimum activation conditions for the catalysts. The peak temperatures in the β ranges could be sufficient activation temperature under CO flow but activation of Fe–Zn–Cu and Fe–Zn–Cu–Ca is like to give more active catalysts because of their lower reduction temperatures under hydrogen flow.

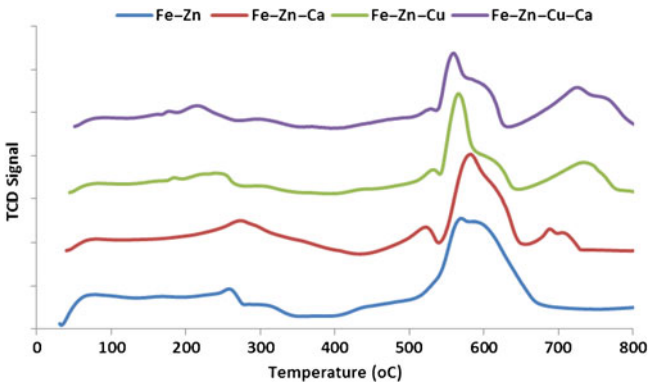

Figure 4. CO–TPR profiles of the catalysts.

3.5 *NH_3-TPD of the catalysts*

In addition to their influence on reduction temperature, Cu and alkali or alkaline metal ions have been indicated to alter surface acid–base properties of Fe oxide precursors which in turn affect the FT product selectivity of the catalysts.[27] NH_3-TPD is one of the techniques for characterizing surface acidity of heterogeneous catalysts. NH_3-TPD profile of the catalysts is presented in figure 6.

The peak temperatures and amount of NH_3 desorbed under the peaks are the indicators of the strength and density of acidic sites on the catalysts. The profile of catalysts is partitioned into weak, medium and strong sites. The effect of Cu and Ca promotion

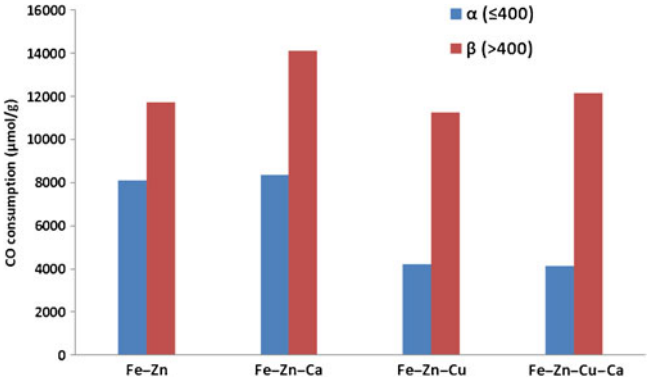

Figure 5. CO consumption measured by area under the peak in different temperature ranges in the CO–TPR profiles of the catalysts.

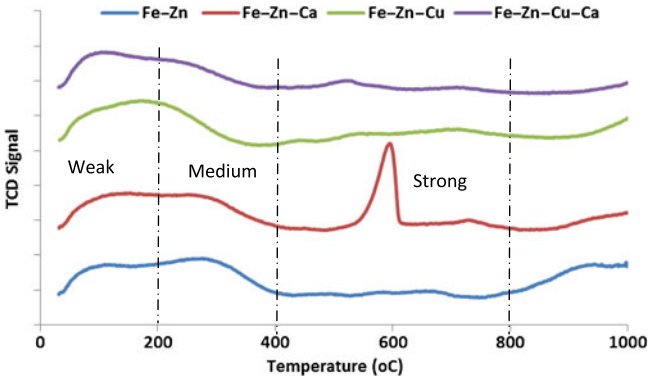

Figure 6. NH_3–TPD profiles of the catalysts.

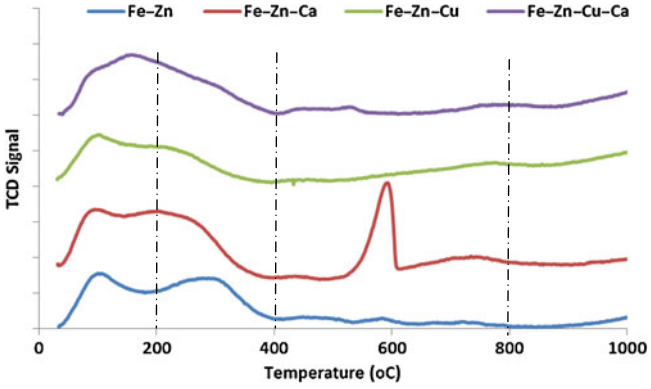

Figure 8. CO_2–TPD profiles of the catalysts.

of Fe–Zn oxide precursor is illustrated in figure 7. Figure 7 showed that total sites densities of Fe–Zn and Fe–Zn–Ca were about the same, however, when compared with Fe–Zn, the proportion of strong sites in Fe–Zn–Ca increase at the expense of medium sites. Alkali and alkaline metal promoter usually impact surface basicity and/or decrease surface acidity of iron-base FT catalysts. Hence, the distribution of the acid sites on Fe–Zn–Ca is rather unexpected. It is note worthy that a similar sharp peak appeared in the CO_2–TPD profiles (figure 8) of Fe–Zn–Ca at the same temperature having the same shape and about the same amount of desorbed gas. This suggests that this peak is intrinsic to the catalyst and not due to desorption of adsorbed NH_3 or CO_2 on the catalyst.

As explained in section 3.2, iron and zinc nitrates precipitate as hydroxides. The hydroxides transformed into α-Fe_2O_3 and $ZnFe_2O_4$ phases after calcination and these phases are stable at high temperatures as NH_3- and CO_2–TPD profiles of Fe–Zn catalyst did show any peak at temperature the sharp peak appeared in Fe–Zn–Ca. Although information about the nature of phase in which Ca is present could not be obtained from XRD,

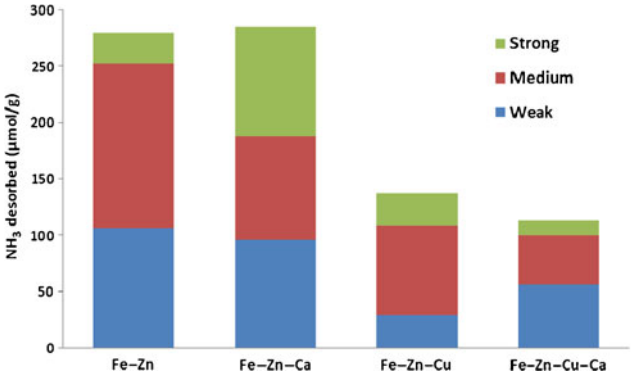

Figure 7. Amount of NH_3 desorbed measured by area under the peak in different temperature ranges in the NH_3-TPD profiles of the catalysts.

we suspect that the sharp peak is connected with the Ca phase in the catalyst. Possible Ca phases in the catalyst are: CaO, $Ca(OH)_2$ and $CaCO_3$. The temperature of the sharp peak is very close to the decomposition temperature of $Ca(OH)_2$. Thus, we suspect that Ca is most probably present as $Ca(OH)_2$ phase and the peak is not due to NH_3 desorbed from strong acidic sites on the catalyst, but most likely due to water molecules released from decomposition of entrapped $Ca(OH)_2$. On the other hand, Cu appears to titrate the acid sites bringing about weakening of the acid strength and decreased in the total acid sites. Co-promotion with Cu and Ca appears to lead to a synergistic effect in further weakening the acid strength and reduction in the total acid sites in Fe–Zn. Acid sites of FT catalysts had been linked to light hydrocarbon selectivity. Increasing surface acid strength and density promotes acid catalysed reactions such as cracking and isomerization.[28,29] According to Snel,[30] branched FT products are mainly formed during secondary isomerization reactions and extent of branching is a function of the catalyst formulation. High acidity and a low hydrogenation strength of the catalyst favour branching. Hence, the extent of branching in the FT products of the catalysts may be expected to follow this order: Fe–Zn–Ca > Fe–Zn > Fe–Zn–Cu > Fe–Zn–Cu–Ca.

3.6 *CO_2–TPD of the catalysts*

As discussed in section 3.5 for NH_3-TPD, CO_2-TPD peak temperatures and amount of desorbed CO_2 are measures of the strength and density of surface basicity of the catalysts. Figure 8 shows the CO_2-TPD profiles partitioned into weak, medium and strong sites and the sites distribution is presented in figure 9. Also, as discussed in section 3.5, a rather identical sharp peak appeared in the NH_3- and CO_2-TPD profiles of Fe–Zn–Ca. Literally the peak should have been

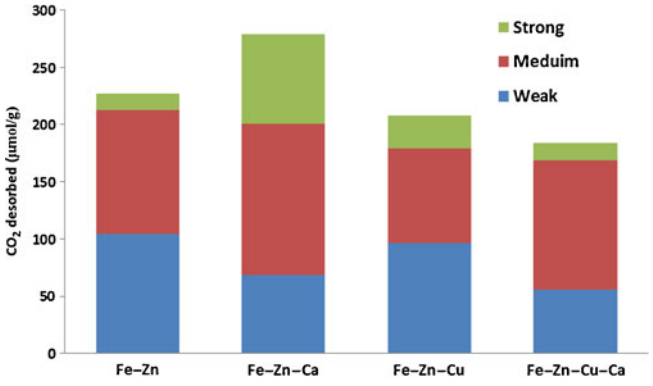

Figure 9. Amount of CO_2 desorbed measured by area under the peak in different temperature ranges in the CO_2–TPD profiles of the catalysts.

interpreted as due to strong sites in each case. But the peak was suspected to be due to decomposition of entrapped $Ca(OH)_2$. The entrapped $Ca(OH)_2$ can function as basic sites in Fe–Zn–Ca. Figure 9 shows that the surface basicity of Fe–Zn is made up of predominantly and about equal amount of weak and medium sites. Comparison of figures 5 and 9 shows that the extent of carburization increases with increasing strength and density of surface basicity of the catalysts. This agrees with common trend in Fe based FT catalysts. The presence of Ca in Fe–Zn not only creates strong basic sites, but also increases the total sites densities in Fe–Zn–Ca. However, addition of Cu to Fe–Zn resulted in slight decrease in the surface basicity and a small increase in the proportion of strong basicity. Similar enhancement of surface basicity on Fe–Mn–K–SiO_2 oxide precursor promoted with Cu was reported by Zhang *et al.*[20] However, co-promotion of Fe–Zn with Cu and Ca leads to a decrease in total surface basicity but with redistribution in favour of medium strength basic sites. The beneficial effect of surface basicity in Fe-based FT catalytsts is well documented. The choice of promoters for Fe-FT catalyst is often guided by their ability to exhibit complementary basicity effect in the catalysts.[31] High surface basicity enhances CO adsorption and dissociation but lowers the hydrogenation strength of Fe catalysts. This results in low methane selectivity and higher C_{5+} selectivity.[32] This explains the similarity of the trends in figures 5 and 9. However, high surface basicity can promote isomerization of alkenes[30] and report by Cubeiro *et al.*[33] indicated that K may promote deactivation of Fe catalysts by re-oxidation. Moreover, lowered the hydrogenation strength and enhanced CO adsorption and dissociation can lead excessive carbon deposition and formation of inactive iron carbide phases and graphitic type carbonaceous surface species, and consequently leads to catalyst deactivation.[34] Thus, the decreased in basicity with Cu and Cu–Ca promotion of Fe–Zn might be beneficial in enhancing stability of the catalyst.

4. Conclusion

We identified Fe–Zn based Fischer–Tropsch catalysts as suitable candidates for coal-based electricity-liquid fuel co-production. We examined effect of Cu and Ca promotion on reducibility, carburization and surface acidity–basicity of the Fe–Zn catalysts using TPR (H_2 and CO) and TPD (NH_3 and CO_2) techniques. Results of the characterization studies provide prior information on expected catalytic behaviour of the catalysts. Ca promotion enhances carburization but Cu inhibits carburization. Enhanced carburization suggests Ca promoted catalyst exhibits high olefins/paraffins ratio, increased C_{5+} selectivity and decreased methane selectivity. A reverse selectivity is expected for Cu promoted catalyst. Surface acidity and basicity increased in the Ca promoted catalyst, while Cu promoted catalyst showed decreased surface acidity and basicity. It suggests that the primary products of Ca promoted catalyst are more prone to acid–base catalysed secondary reactions than in the Cu promoted catalyst. The independent effects of Cu and Ca promotion may result in a synergy in Cu–Ca co-promoted catalyst.

Acknowledgements

S Maity and O O James thank the Director, Central Institute of Mining and Fuel Research (CIMFR) for permitting to publish this paper. O O James thanks TWAS (Triestie, Italy) and CSIR (India) for the award of TWAS-CSIR Postgraduate Fellowship. The authors also thank Dr. E R Masto of EMD Department, CIMFR, Digwadih Campus, for assistance with ICP-OES analysis of the catalyst samples.

References

1. James O O, Mesubi M A, Ako T C, Maity S 2010 *Fuel Process. Technol.* **91** 136
2. Traa Y 2010 *Chem. Commun.* **46** 2175
3. de Smit E, Weckhuysen B M 2008 *Chem. Soc. Rev.* **37** 2758
4. Dry M E 2002 *Catal. Today* **71** 227
5. Schulz H 1999 *Appl. Catal. A-Gen.* **186** 3
6. David A W, Chikezie N, Brian F T 2012 *J. Nat. Gas Sci. Eng.* **9** 196
7. Chen Y H H, Reilly J M, Paltsev S 2011 *Energy Policy* **39(9)** 4713
8. Fang R, David G V 2011 *Energy Policy* **39(12)** 8175

9. Frederik T, Magnus F, Frank S, Ralph S, Edmund H 2011 *Fuel Process. Technol.* **92** 2169
10. Sunde K, Brekke A, Solberg B 2011 *For. Policy Econ.* **13(8)** 591
11. Dry M E 2004 *studies in surface science and catalysis 152: Fischer–Tropsch technology* (eds) A P Steynberg and M Dry (Elsevier, Amsterdam) pp. 196–257
12. Dry M E 2001 *J. Chem. Technol. Biotechnol.* **77** 43
13. Klerk A D 2009 *Energy Fuel* **23** 4593
14. Liu G, Larson E D, Williams R H, Kreutz T G, Guo X 2011 *Energy Fuels* **25** 415
15. James O O, Chowdhury B, Mesubi M A, Maity S 2012 *RSC Adv.* **2** 7347
16. Li S, Krishnamoorthy S, Li A, Meitzner G D, Iglesia E 2002 *J. Catal.* **206** 202
17. O'Brien R J, Davis B H 2004 *Catal. Lett.* **94(1–2)** 1
18. Yang Y, Xiang H-W, Xu Y-Y, Bai L, Li Y-W 2004 *Appl. Catal. A: Gen.* **266** 181
19. Wan H, Wu B, Zhang C, Xiang H, Li Y 2008 *J. Mol. Catal. A: Chem.* **283** 33
20. de Smit E, de Groot F M F, Blume R, Havecker M, Knop-Gericke A, Weckhuysen B M 2010 *Phys. Chem. Chem. Phys.* **12** 667
21. Li S, Li A, Krishnamoorthy S, Iglesia E 2001 *Catal. Lett.* **77(4)** 197
22. Luo M, Davis B H 2003 *Appl. Catal. A-Gen.* **246** 171
23. Pour A N, Shahri S M K, Bozorgzadeh H R, Zamani Y, Tavasoli A, Marvast M A 2008 *Appl. Catal. A: Gen.* **348** 201
24. Yuvaraj S, Fan-Yuan L, Tsong-Huei C, Chuin-Tih Y 2003 *J. Phys. Chem. B* **107** 1044
25. Brockner W, Ehrhardt C, Gjikaj M 2007 *Thermochim. Acta* **456** 64
26. Tao Z, Yang Y, Zhang C, Li T, Wang J, Wan H, Xiang H, Li Y 2006 *Catal. Commun.* **7** 1061
27. Zhang C-H, Yang Y, Teng B-T, Li T-Z, Zheng H-Y, Xiang H-W, Li Y-W 2006 *J. Catal.* **237** 405
28. Wan H-J, Wu B-S, An X, Li T-Z, Tao Z-C, Xiang H-W, Li Y-W 2007 *J. Nat. Gas Chem.* **16(2)** 130
29. Pour A N, Zamani Y, Tavasoli A, Shahri S M K, Sayyed A T 2008 *Fuel* **87(10–11)** 2004
30. Snel R 1989 *J. Mol. Catal.* **50(1)** 103
31. Snel R 1988 *Appl. Catal.* **37** 35
32. Graf B, Schulte H, Muhler M 2010 *J. Catal.* **276(1)** 66
33. Cubeiro M L, Morales H, Goldwasser M R, Pérez-Zurita M J, González-Jiménez F 2000 *React. Kinet. Catal. L.* **69(2)** 259
34. Pour A N, Housaindokht M R, Zarkesh J, Tayyari S F 2010 *J. Ind. Eng. Chem.* **16(6)** 1025